Biochimica et Biophysica Acta, 1103 (1992) 317–323

BBAMEM 75502

Homeoviscous adaptation under pressure: the pressure dependence of membrane order in brain myelin membranes of deep-sea fish

M.K. Behan [1], A.G. Macdonald [2], G.R. Jones [3] and A.R. Cossins [1]

[1] *Environmental Physiology Research Group, Department of Environmental and Evolutionary Biology, University of Liverpool, Liverpool (UK),* [2] *Department of Physiology, Marischal College, University of Aberdeen, Aberdeen, Scotland (UK) and* [3] *Biology Support Laboratory, S.E.R.C. Laboratory, Daresbury, Cheshire (UK)*

(Received 30 July 1991)

Key words: Fluorescence anisotropy; DPH; Myelin; Membrane fluidity; Pressure adaptation; Homeoviscous adaptation

Steady-state and time-resolved anisotropy of 1,6-diphenyl-1,3,5-hexatriene (DPH) fluorescence have been used to compare the hydrocarbon order of brain myelin membranes from a shallow water (plaice) and two deep-sea fish species (*Coryphenoides rupestris* and *Coryphenoides armatus*). At atmospheric pressure the deep sea fish displayed lower steady-state anisotropies than shallow water species although the pressure dependence of anisotropy was similar in all species. Time-resolved measurements allowed the separate determination of the rate of probe motion from the amplitude of that motion. Anisotropy decays were analysed in terms of two correlation times and a constant (r_∞). The r_∞ and $\langle P_2 \rangle$ order parameter for all species increased with pressure, the graphs for deep-sea species being translated to higher pressures relative to shallow-water species. The resulting pressure coefficients for *C. armatus* was distinctly less than for the two shallower species. These time-resolved studies show that the interspecific differences provide for similar order parameters in all three species when corrected to their respective habitat conditions of pressure and temperature. This indicates that myelin order is highly conserved despite the profound ordering effects of high hydrostatic pressure.

Introduction

Hydrostatic pressure greatly influences the structural properties and functional characteristics of biological membranes, yet this has not prevented the invasion of high pressure, cold habitats (up to 10000 m depth, ≈ 1 kbar, 2–3°C) by deep-sea organisms, including fish. In general, increased pressure raises membrane phase transition temperatures and enhances the order of hydrocarbon chains [1] in much the same way as cooling to the extent that 1000 atm and 2°C is equivalent in its ordering effects to approximately −18°C at atmospheric pressures [2,3]. Without any compensatory adjustment the membranes of deep-sea organisms should be highly ordered. It is now well established that deep-sea fish display a variety of adaptations to high hydrostatic pressures at the cellular and molecular level of organization [4], including adjustments of the lipid composition and hydrocarbon order of cellular membranes [5–7].

In principle, there are two extreme forms of membrane adaptation for the ordering effects of hydrostatic pressure. Firstly, the membranes of deep-sea organisms may show a reduced pressure sensitivity compared with shallow-water species and, secondly, they may possess similar pressure sensitivities but a lower lipid order compared to shallow-water species. In both cases the differences between deep-sea and shallow-water species would offset the direct ordering effects of pressure though by rather different mechanisms.

Although previous studies have provided evidence in favour of the pressure adaptation of membranes from deep-sea fish species [5] the pressure dependence of membrane order was not measured. To rectify this we have determined the pressure dependence of fluo-

Abbreviation: DPH, 1,6-diphenyl-1,3,5-hexatriene.

Correspondence: A.R. Cossins, Environmental Physiology Research Group, Department of Environmental and Evolutionary Biology, University of Liverpool, P.O. Box 147, Liverpool L69 3BX, UK.

rescence anisotropy of the probe 1,6-diphenyl-1,3,5-hexatriene (DPH) in myelin membranes from deep-sea and surface-dwelling fish species using both steady-state and time-resolved methods. We have selected for study two species from the genus *Coryphenoides* which inhabit different depth ranges down to at least 4000 m and compared them to plaice. The results indicate that a simple translational adaptation occurs at moderate depths but that in the deep-sea species *C. armatus* there is some evidence of a reduction in pressure dependence. The net effect is that hydrocarbon order is similar in all three species when determined at their respective ambient conditions of temperature and hydrostatic pressure.

Materials and Methods

Materials

Trans-1,6-diphenyl-1,3,5-hexatriene (DPH) was purchased from Aldrich Chemical Co. and was 'Puriss' grade. Tetrahydrofuran was obtained from BDH Chemicals Ltd., Poole, Dorset and was analytical reagent grade.

Animals

Deep-sea fish were obtained in September 1985 during a cruise on R.R.S. Challenger to the Porcupine Sea Bight off southwestern Ireland (approx. 50°N, 13°W). Two species were selected; *Coryphenoides rupestris* and *C. armatus*. They were trawled using a semi-balloon otter trawl at 900 m and 4000 m, respectively. Plaice (*Pleuronectes platessa*) were obtained in the North Sea and kept in a seawater aquarium at 9°C for several weeks.

Preparation of brain membranes

Membranes from deep-sea fish were prepared on board ship from fish immediately upon landing. Brains of several specimens were dissected out, freed of adhering fatty material and homogenized in 2 ml of ice-cold isolation medium (320 mM sucrose, 2 mM ethylenediaminetetraacetic acid, 30 mM imidazole (pH 7.4) at room temperature) using a glass-teflon homogeniser. The homogenate was centrifuged at $1000 \times g$ for 10 min. The supernatant was removed and centrifuged at $15000 \times g$ for 30 min in a Centra 3R-S refrigerated centrifuge (Damon-IEC). The pellet was resuspended in lysing medium (10 mM imidazole, 1 mM ethylenediaminetetraacetic acid (pH 7.4)) using a close fitting glass-glass homogeniser (Kontes 'A' pestle) and recentrifuged at $15000 \times g$ for 30 min. The resulting pellet was resuspended in 4 ml lysing medium and layered on a cushion of 3 ml 0.8 M sucrose, 10 mM imidazole (pH 7.4) and centrifuged at $15000 \times g$ for 60 min. Brain myelin fraction was collected at the interface of the lysing and sucrose solutions using a Pasteur pipette, diluted with 3 vols. (v/v) lysing medium and centrifuged at $15000 \times g$ for 30 min. The resulting pellet was resuspended in approximately 0.4 ml lysing medium and stored at −20°C for several days and −80°C for up to 12 months. Myelin membranes from plaice were prepared similarly but in the laboratory.

Fluorescence anisotropy measurements

Myelin membrane preparations were diluted with 2 mM phosphate buffer (pH 7.6, room temperature) to give an absorbance of 0.1 at 500 nm. They were labelled by addition of 2 μl DPH (2 mM in tetrahydofuran) to 3 ml of membrane suspension (probe/lipid ratio of 1:500) and incubated at room temperature for at least 20 min.

Steady-state anisotropy was determined on the T-format instrument described previously [6]. Anisotropy versus temperature scans for DPH were repeated and reproducible, giving anisotropy values within ±0.005. Limited supplies of deep-sea material prevented duplicate measurements being made. Measurements were undertaken at pressures up to 1 kbar with the high pressure vessel described previously [6]. Samples were sealed in a cylindrical quartz cuvette and separated from the pressure-transmitting fluid, ethanol, by a silicon diaphragm. The temperature of the vessel was controlled to ±0.1°C by pumping water from a Julabo refrigerated thermocirculator through channels drilled in the steel walls of the vessel. The sample temperature was indirectly monitored by a linear thermistor or platinum resistance thermometer inserted into the wall of the pressure vessel. Correction for strain birefringence of the three quartz windows under pressure was made using the fluorescein technique [8]. As the correction factor was wavelength-dependent it was necessary to determine it at the excitation wavelength used for DPH (360 nm).

Time-resolved anisotropy measurements were performed using the high aperture port (HA12) of the synchrotron radiation source at S.E.R.C. Daresbury Laboratory, Warrington, U.K., working in single bunch mode at 3MHz. The single photon-counting apparatus was an L-format fluorimeter with a Philips XP 2020Q photomultiplier as detector and a conventional TAC-based timing system. The same pressure vessel was mounted and aligned in the usual way. Corrections for strain birefringence of the two quartz windows of the L-format were made using the method of Paladini [9] as modified for anisotropy by Jones, G.R.. Fluorescein was used at an excitation wavelength of 360 nm. For anisotropy measurements the parallel and perpendicular components of the fluorescence decay were collected alternately into two 1024-channel memory banks of a multichannel analyser by rotating the analyser polarizer every 100 s over 10 periods. The total fluorescence decay was measured by combining the parallel

and perpendicular components of the fluorescence emission for each time interval on the multichannel analyser. Anisotropy was calculated by dividing the difference between the parallel and perpendicular components by the total fluorescence. Computer programmes to fit different models to the anisotropy decay and fluorescence decay curves were provided by Daresbury Laboratory. The anisotropy decay data were characterized by non-linear least squares analysis of the following equations;

(1) A sum of exponentials

$$r(t) = \sum_i b_i \, e^{(-t/\phi_i)}$$

where ϕ_i are the rotational correlation times. The sum of the pre-exponential terms (b_i) represents the emission anisotropy at time zero.

(2) A sum of exponentials plus an r_∞ term

$$r(t) = r_\infty + \sum_i b_i \, e^{(-t/\phi_i)}$$

where r_∞ represents the residual anisotropy at times long compared to the fluorescence lifetime of the probe.

The computer program was based on a Marquardt minimisation of the non-linear, least-squares fit [10], having first convoluted the instrumental response individually to the sum and difference term. Synchrotron radiation allows the instrumental response to be recorded at the same wavelength as the fluorescence emission, thus reducing the 'colour' effects or transit time artefacts of the photomultiplier tube. Goodness of fit was assessed by a reduced chi squared (χ^2) of close to unity and totally random residuals using standard methods [11]. The inability to remove all scattered light during the high pressure measurements resulted in a short-lived, scattered-light component. This was extracted from the data by including in the curve-fitting analysis a short component of fixed correlation time (approximately 0.01 ns) but floating pre-exponential factor. In this way the calculated r_0 was found to be relatively constant at 0.322 ± 0.010 (median ± range).

The second rank order parameter, $\langle P_2 \rangle$, from electron spin resonance measurements is related to r_∞ from time-resolved anisotropy measurements [12,13] by

$$r_\infty / r_0 = \langle P_2 \rangle^2$$

where r_0 is the anisotropy before any rotation has taken place ($t = 0$). The diffusion coefficient ($D_\perp$) was calculated according to Ameloot et al. [14] by an extension of the simpler model-independent interpolation of Lipari and Szabo [15]

$$D_\perp = \frac{1}{6 r_0} \sum_i \frac{b_i}{\phi_i}$$

where b_i was the pre-exponential factor and ϕ_i was the rotational correlation time. For all cases r_0 was calculated from:

$$r_0 = b_i + r_\infty$$

after extraction of the pre-exponential factor representing the scattered light component.

Due to the strictly limited amount and unique nature of material available from deep-sea fish species, measurements were only possible on one preparation from each species. Problems with the thermal equilibration of the pressure vessel meant that time-resolved measurements for *C. armatus* were performed at 8.0 ± 0.1°C instead of 4.0 ± 0.1°C used for other species. The limiting anisotropy (r_∞) at 8°C was corrected to 4°C by reference to the effects of temperature upon steady-state anisotropy. Preliminary experiments indicated that the pressure coefficient at 8 and 4°C was identical so the percentage change in r_∞ determined at atmospheric pressure was used.

Typical experimental errors can be gauged from replicate analyses of goldfish brain synaptic membrane at 15°C which were analysed according to the two correlation time plus r_∞ model used for the marine species. Mean ± S.D. for b_1 was 0.063 ± 0.005 ($n = 4$), whilst the corresponding values for ϕ_1 was 0.79 ± 0.292 ns, b_2 was 0.066 ± 0.010, ϕ_2 was 3.964 ± 0.292 and r_∞ was 0.205 ± 0.003. Chi-squared values were in the range 1.017–1.040.

Graphs have been drawn using a commercial graphics package. The lines in Figs. 1 and 3 represent computer generated fits using polynomial or linear equations.

Results

Fig. 1 shows the effects of hydrostatic pressure upon steady-state anisotropy of DPH in myelin membranes at 4°C. Anisotropy in membranes from *C. armatus* was substantially lower than those from *C. rupestris* which in turn was lower than those of plaice membranes. This is consistent with a previously observed relationship of DPH anisotropy with depth of capture [6]. All species showed approximately linear dependencies upon pressure with a regression coefficient of between 0.025 ± 0.002 and 0.036 ± 0.002 anisotropy units per kbar (mean ± S.E.). Values obtained during decompression were similar (data not shown) to those obtained during compression indicating that the effects of pressure were entirely reversible.

The fluorescence lifetimes for DPH in myelin membranes were determined from the decay of the fluorescence intensity (data not shown). The decay curves for plaice and *C. rupestris* were collected at 4°C and because of instrumental difficulties those for *C. armatus*

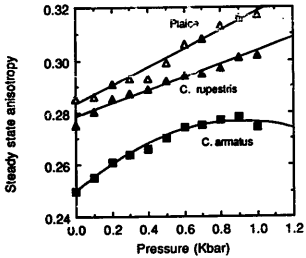

Fig. 1. The effects of hydrostatic pressure upon the steady-state anisotropy of DPH in brain myelin membranes from plaice, *C. rupestris* and *C. armatus*. Values were determined at 4°C. Curves for plaice have been repeated and found to be reproducible within 0.005 anisotropy units.

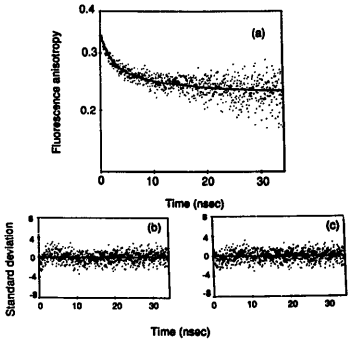

Fig. 2. (a) A typical anisotropy decay curve fitted using a double-exponential plus r_∞ decay law for DPH in brain myelin membranes of plaice at atmospheric pressure and 4°C. The associated standard deviation of residuals for different models to the decay data are shown below: (b) double-exponential, (c) double-exponential plus r_∞.

were collected at 8°C. The decays for most species were best fitted by a tri-exponential decay law with the exception of plaice where a bi-exponential decay law was found to be adequate. The short component of the triple-exponential fit was probably due to scattered light, which because of the relatively large membrane vesicles and fragments proved particularly difficult to remove. The weighted mean lifetime showed a monotonic decrease with increasing pressure.

The time-dependence of the anisotropy decay was analysed using a number of different mathematical models as described in Materials and Methods. The reduced chi-squared test and analysis of residuals (Table I and Fig. 2, respectively) indicated that, after extracting the scattered light component, the data was equally well described by the bi-exponential decay law plus a constant (r_∞) and by the tri-exponential decay law. For the purposes of comparing the decays of different species the former model was used (Table I) because: (1) It contained one less variable. (2) The third component of the tri-exponential decay was invariably 25–30-times greater than the fluorescence lifetime of the probe used and practically indistinguishable from an infinite term.

Curve fitting with the bi-exponential decay plus r_∞ led to calculated values of r_0 which ranged from 0.312 to 0.342 with a median of 0.327 with no obvious relationship with pressure or between species (data not shown).

TABLE I

Comparison of the fluorescence anisotropy decay parameters for DPH in brain myelin membranes from plaice obtained using different mathematical models

Model 1 was a double-exponential decay plus an r_∞, Model 2 was a single-exponential decay plus r_∞, Model 3 was a double-exponential and Model 4 was a triple-exponential decay. ϕ_1, ϕ_2 and ϕ_3 were rotational correlation times and b_1, b_2 and b_3 were the corresponding pre-exponential constants. For simplicity, curves were fitted from MCA channels after the early scattered component had decayed.

Pressure (kbar)	Model	χ^2	b_1	ϕ_1	b_2	ϕ_2	b_3	ϕ_3	r_∞
0.001	1	1.07	0.07	1.76	0.049	12.82			0.224
0.001	2	1.53			0.110	1.99			0.244
0.001	3	1.15			0.097	1.30	0.26	183	
0.001	4	1.08	0.24	0.02	0.080	2.50	0.25	278	
0.800	1	1.19	0.02	1.15	0.045	8.02			0.274
0.800	2	1.28			0.060	5.99			0.275
0.800	3	1.31			0.065	1.50	0.299	314	
0.800	4	1.24	0.82	0.02	0.050	2.81	0.290	363	

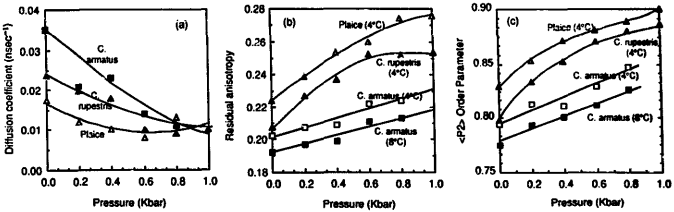

Fig. 3. The effects of hydrostatic pressure upon (a) the rotational diffusion coefficient ($D_\perp$), (b) r_∞ and (c) the order parameter $\langle P_2 \rangle$ for DPH in brain myelin membranes from plaice and *C. rupestris* at 4°C and from *C. armatus* at 8°C. In (b) and (c) the estimated position of the curves at 4°C is also shown, the values being corrected for the small temperature difference as described in the Methods.

The rotational correlation times showed no consistent interspecific differences (data not shown). Fig. 3(a) shows the dependence of the diffusion coefficient upon pressure, with increasing pressure resulting in a progressive decrease in diffusion coefficient. For pressures up to 0.6 kbar the diffusion coefficients were greatest in membranes from *C. armatus* and least in membranes from plaice indicating an interspecific difference which corresponded to their respective depth ranges. At higher pressures there was no difference between species.

Fig. 3(b) shows the effects of pressure upon r_∞. Because the data for *C. armatus* was collected at 8°C it was necessary for the proper comparison of species to estimate the position of the curve for *C. armatus* at 4°C (see Methods). The r_∞ term increased in the order *C. armatus* < *C. rupestris* < plaice. *C. armatus* showed a linear increase in r_∞ with increasing pressure. By contrast, *C. rupestris* and plaice showed distinctly curvilinear graphs with pressure exerting a greater effect over the lower pressure range. The calculated values for the order parameter, $\langle P_2 \rangle$, are illustrated in Fig. 3(c) again with a curve representing *C. armatus* at 4°C. As before *C. armatus* showed a linear increase with increasing pressure whilst the slopes for the other species were curvilinear. By comparing the curves for each species at 4°C it is clear that the position of the curve for *C. armatus* was shifted to lower $\langle P_2 \rangle$ values relative to *C. rupestris*. Similarly, the curve for *C. rupestris* was shifted to lower $\langle P_2 \rangle$ values compared to plaice.

Discussion

The comparison of myelin membranes from different species using steady-state anisotropy indicates that membranes of *C. armatus* were more disordered than *C. rupestris* and these were more disordered than plaice. These interspecific differences and the actual anisotropies are entirely consistent with a previous study in which DPH polarization in myelin membrane fractions was significantly correlated with depth of capture [5]. This conclusion is important because it indicates that the membrane preparations used in the present study were typical of their respective species. Moreover, the interspecific differences were exactly that expected from a straightforward compensatory difference between species. The similar pressure dependencies of steady-state anisotropy indicates a straightforward translational difference between membranes of the deep-sea species and those of plaice. The shift of the curves along the pressure axis was more than sufficient to provide similar anisotropies for each species over their respective ambient pressure ranges.

Adjustment of membranes to altered temperature during thermal acclimation is also achieved by a translational shift of the curve relating DPH anisotropy to temperature as opposed to a change in temperature dependence. The magnitude of the adjustment has been characterized by the 'homoeoviscous efficacy' [16], which is the extent to which temperature-induced disturbance is offset by adaptations of membrane order. It is simply calculated by measuring the difference in °C of the position of the compared anisotropy/temperature curves on the temperature axis and expressing this as a fraction of the difference in adaptation temperatures. A value of unity indicates that the curves differed by the same temperature interval as the difference in body temperatures, resulting in identical anisotropies at their respective body temperatures.

The same procedure can be adopted with respect to pressure in the case of steady-state anisotropy because of the apparently simple translation of the curves. Thus, the curve relating anisotropy to pressure for *C. rupestris* was shifted by approx. 0.21 kbar with respect to plaice. *C. rupestris* normally occurs over a depth range of 400–2000 m in the North Atlantic (Merrett, N., personal communication) so that the difference in the position of the anisotropy/pressure curves was

sufficient to provide an identical anisotropy for *C. rupestris* at its maximal depth as that found in plaice at pressures characteristic of the surface layers. Homeoviscous efficacy in this case is unity or 100%. The curve for *C. armatus* was shifted by more than 0.6 kbar with respect to plaice. *C. armatus* occurs at depths between 2200–4800 m (Merrett, N., personal communication) so that the difference was somewhat greater than that required to provide identical anisotropies. Homeoviscous efficacy was equal to or greater than 100%.

In contrast to steady-state anisotropy, measuring the time dependence of emission anisotropy provides a direct means of distinguishing between the orientational order and rate of rotational motion of probe [14,17]. We have found no clear or consistent interspecific difference in the rotational correlation times which relates to their different environmental pressures. The interspecific difference in rotational diffusion coefficient shown in Fig. 3 originates from the relative contributions of r_∞ and the pre-exponential terms to r_0, rather then from a direct effect of rotational rate. Regarding the pressure dependence of the rotational diffusion coefficient, a previous time-resolved study showed that the rotational rate and wobbling diffusion coefficient calculated from differential polarized phase measurements showed at high temperatures a decrease with increasing hydrostatic pressure but at low temperatures a surprising increase with increasing pressure [3,18]. By contrast the experiments described here showed a monophasic decrease in the rotational diffusion coefficient with increasing pressure in all three species both at high and low temperatures. It is worth pointing out that the present measurements were directly taken from the anisotropy decay using a model-independent method whilst the earlier phase methods used a model which may be deficient.

Whilst the pressure dependency of steady-state anisotropy was similar in all three species, the time resolved analysis provides evidence of a difference in pressure dependence between *C. armatus* and the two shallower species. The $\langle P_2 \rangle$ order parameter for *C. armatus* showed a linear and shallow increase with pressure whilst for *C. rupestris* and plaice the relationship was steeper and curvilinear. The pressure dependence for *C. rupestris* and plaice over the range 1–200 bar was approximately twice that for *C. armatus* although over the higher range of pressures (400–1000 bar) it was similar to that observed for *C. armatus* over the entire range of pressures. This suggests that the difference between the membranes of plaice and *C. rupestris* was caused by a simple translation of the curves relating membrane order to pressure and whatever the differences in biochemical composition which underlie their different physical properties they do not significantly alter compressibility. On the other hand, the difference between the membranes of *C. rupestris* and *C. armatus* was due to a change in the pressure-dependence of order as well as a change in the extent of hydrocarbon chain order. This implies, firstly, that that variation in lipid composition of these two species is qualitatively different to the variation between plaice and *C. rupestris* and, secondly, that compressibility is reduced in the deep-sea species relative to the two shallower species.

The most important aspect of the time-resolved analysis is the extent to which it supports the conclusions from steady-state analyses regarding the magnitude of the adaptive differences between species. Because of the the curvilinear form of the relationship between r_∞ and pressure it is not possible to calculate homeoviscous efficacy. Moreover, in that individuals may migrate vertically through the water column it is not possible to define a single depth to which they have become adapted. It is clear from the values of $\langle P_2 \rangle$ order parameter that there were substantial differences between species and that, as with the steady-state comparison, these differences correlated with the depth range inhabited by each species. The curves relating $\langle P_2 \rangle$ order parameter to pressure were displaced with respect to each other with the result that the membranes of each species displayed broadly similar values of $\langle P_2 \rangle$ order parameter over their respective ambient pressure ranges. Thus, despite the diffcrent pressures experienced by each species the fact that the second rank order parameters for DPH were similar suggests again that the myelin membranes possess similar physical propertics at their respective ambient conditions.

The time-resolved analysis indicates clearly that it is those structural characteristics of the membrane interior which influence the amplitude of DPH wobbling motion, rather than its reorientational rate, that are altered to take account of the increased pressure. As with previous studies relating the characteristics of DPH motion to the local structure of the membrane hydrocarbon interior [14,17,19], this is taken to be evidence of an adjustment to the orientational order of the hydrocarbon chains of the membrane interior by means principally of an adjustment in lipid saturation [6]. In this specific respect the time-resolved analysis fully confirms and extends the steady-state analysis.

Another way of illustrating the adaptive nature of the interspecific differences in order is to calculate the values for $\langle P_2 \rangle$ at identical conditions of temperature and pressure as well as at the respective ambient conditions for each species (Table II). At 4°C and atmospheric pressure the values of $\langle P_2 \rangle$ of the three marine species varied from 0.794 to 0.829 whilst at their respective ambient conditions of temperature and pressure $\langle P_2 \rangle$ for the deep-sea species (0.811–0.813) was almost identical to that of plaice (0.807). This again provides evidence that adaptation of these two deep-sea species to their high pressure habitat involved

TABLE II

Comparison of the order parameters for DPH in brain myelin membranes of deep-sea and shallow-water species at their respective ambient temperatures and pressures

Values of r_x illustrated in Fig. 3(b), were corrected to the conditions of temperature and pressure specified in the Table as described in the Methods. $\langle P_2 \rangle$ values were then calculated from these corrected values of r_x.

Species	Ambient temperature (°C)	Ambient pressure (kbar)	Order parameter $\langle P_2 \rangle$		
			Atmospheric pressure &4°C	Ambient pressure &4°C	Ambient pressure &temperature
Plaice	9	0.001	0.829	0.829	0.807
C. rupestris	4	0.090	0.799	0.811	0.811
C. armatus	3	0.400	0.794	0.808	0.813

a shift in membrane properties which was sufficiently great to offset completely the direct ordering effects of high pressure.

Thus the interspecific differences are sufficiently great to provide for broadly similar membrane orders in the three species *at their respective ambient pressures*. Adaptation occurs largely by a translational shift of the membrane order/pressure curves although there may be some reduction in the effects of pressure upon membrane order in deep-sea fish.

Acknowledgements

We wish to thank the Master and crew of R.R.S. Challenger, Dr. N. Merrett for confirming the identity of the deep-sea fish, Dr. C.S. Wardle for providing plaice, Prof. R.B. Cundall and Dr. J.T. Richards for the use of high pressure equipment and Tana Green and Valerie McDiarmid for technical assistance on Challenger. This work was supported in part by grants from N.E.R.C. to A.G.M. and from S.E.R.C. to A.R.C. and G.R.J.

References

1 Macdonald, A.G. (1987) in Current Perspectives in High Pressure Biology, (Jannasch, H.W., Marquis, R.E. and Zimmerman, A.M., eds.), pp. 207–223, Academic Press, London.
2 Macdonald, A.G. and Cossins, A.R. (1985) in Physiological Adaptations of Marine Animals (Laverack, M.S., ed.), pp. 301–322, Company of Biologists Ltd., Cambridge.
3 Chong, P.L.-G., Cossins, A.R. and Weber, G. (1983) Biochemistry 22, 409–415.
4 Somero, G.N. (1991) in Environmental and Metabolic Animal Physiology, (Prosser, C.L., ed.), pp. 167–204, Wiley-Liss, New York.
5 Cossins, A.R. and Macdonald, A.G. (1989) J. Bioeng. Biomembr. 21, 115–135.
6 Cossins, A.R. and Macdonald, A.G. (1984) Biochim. Biophys. Acta 776, 144–150.
7 Gibbs, A. and Somero, G.N. (1990) J. Comp. Physiol. 160, 431–439.
8 Paladini, A.A. and Weber, G. (1981) Rev. Sci. Instrum. 52, 419–427.
9 Paladini, A.A. (1980) Ph.D Thesis, University of Illinois, Urbana, IL
10 Marquardt, D.W. (1963) J. Soc. Indust. Appl. Math. 11, 431–467.
11 Bevington, P.V. (1969) Data Reduction and Error Analysis for the Physical Sciences, McGraw-Hill, New York.
12 Heyn, M.P. (1979) FEBS Lett. 108, 359–364.
13 Jahnig, F. (1979) Proc. Natl. Acad. Sci. USA 76, 6361–6365.
14 Ameloot, M., Hendrickx, H., Herreman, W., Pottel, H., Van Cauwelaert, F. and Van der Meer, W. (1984) Biophys. J. 46, 525–539.
15 Lipari, G. and Szabo, A. (1980) Biophys. J. 30, 489–506.
16 Cossins, A.R. (1983) in Cellular Acclimatisation to Environmental Change (Cossins, A.R. and Sheterline, P.S., eds.), pp. 3–32, Cambridge University Press, Cambridge.
17 Van der Meer, W., Pottel, H., Herreman, W., Ameloot, M. and Hendrickx, H. (1984) Biophys. J. 46, 515–523.
18 Lakowicz, J.R. and Thompson, R.B. (1983) Biochim. Biophys. Acta 732, 359–371.
19 Van der Meer, W. (1984) in Physiology of Membrane Fluidity (Shinitzky, M., ed.), pp. 53–72, CRC Press, Boca Raton.